*In "Self-sustaining mechanisms of wall-bounded turbulence," R.L. Panton, Editor. Computational Mechanics Publications, 1997.* (96/8/31).

# How streamwise rolls and streaks self-sustain in a shear flow

**Fabian Waleffe[1] and John Kim[2]**

[1]*Department of Mathematics, MIT, Cambridge, MA 02139, USA*

[2]*Department of Mechanical and Aerospace Engineering, UCLA, Los Angeles, CA 90095-1597, USA*

**Abstract**

Using a combination of constrained numerical simulations, stability analysis and low-order dynamical systems, a generic self-sustaining process in shear flows has been isolated. The process consists of streamwise rolls that redistribute the streamwise momentum to create streaks whose wake-like instability nonlinearly maintains the rolls. The identification of this process was inspired by observations of coherent structures in turbulent boundary layers and earlier theoretical work. The process has been isolated at transitional Reynolds numbers, where it occupies the full channel in plane Couette flow. The lowest Reynolds number for stable self-sustenance corresponds to the critical Reynolds number for transition. At higher Reynolds number, it is speculated that the same process is confined to the buffer layer and that the critical parameters for its self-sustenance control the buffer layer thickness and the near-wall streak spacing.

# 1 Introduction

Turbulence in wall-bounded shear flows is strongly controlled by the near-wall region, which is where most of the turbulence energy production and dissipation take place. The ubiquitous structural features in this region are low- and high-speed "streaks" and streamwise vortices. The streaks, which consist mostly of a spanwise modulation of the streamwise velocity, have a characteristic average spacing of about 100 wall units [1] (Kline *et al.* 1967, Smith & Metzler 1983, Kim *et al.* 1987). They have been linked to a sequence of events called the "bursting process," in which streaks lift up, oscillate and break down. The bursting process is believed to be the essence of the turbulence production mechanism (Kim *et al.* 1971). The streaks have also been linked to the genesis of "horseshoe" vortices through a Kelvin-Helmholtz type roll-up (e.g. Acarlar & Smith, 1987). The streaks could in

[1]That is, $100\,\nu/u_\tau$, where $\nu$ is the kinematic velocity and $u_\tau = (\nu|d\overline{U}/dy|_w)^{1/2}$ is the wall-shear velocity. In this paper, $u, v, w$ denote the velocity components in the streamwise ($x$), wall-normal ($y$) and spanwise ($z$) directions, respectively.

turn simply be the wakes left behind the horseshoe vortices as the latter are advected downstream at a speed close to the local mean flow. This is an appealing picture, which not only provides a mutually-sustaining mechanism for the streaks and the horseshoes, but also incorporates interaction with the outer flow. Horseshoes, which are symmetric, are actually less typical than asymmetric, staggered vortices, but from a dynamical viewpoint there is no fundamental difference, except perhaps that the interaction with the outer flow is less clear for asymmetric vortices.

In spite of the attention they have attracted during the past three decades (e.g. see Robinson 1991 for a stereoscopic review), very little is known or agreed upon about the dynamics of streaks and streamwise vortices. There is no consensus, for example, about how such structures are generated and self-sustained nor about what determines their well-known scales. We have learned a great deal about their kinematics but have yet to learn about their dynamics. Understanding of their dynamics is important to the success of modeling and control of turbulent boundary layers.

In light of these earlier studies, we have sought to discover a self-sustaining process in the Navier-Stokes dynamics that is based on the streaks, along the lines of the work by Benney (1984). A simple mechanism for the formation of streaks is the redistribution of the mean shear by streamwise rolls. This advection process creates streaks that are perfectly correlated with the rolls, [2] and the Reynolds stress resulting from the streamwise rolls and streaks then easily maintains a turbulent-like mean profile, at least at low Reynolds numbers (Hamilton, Kim & Waleffe 1995, Waleffe 1995a). In fact, the solenoidal vector field that maximizes the momentum transport (i.e. the total Reynolds stress) has the form of a nested hierarchy of streamwise rolls and streaks (Busse 1970).

It is well-known that the streamwise rolls decay viscously in a purely $x$-independent flow (e.g. Joseph and Tao 1963). The key point, then, is to determine the mechanism by which the streamwise rolls are maintained. Several proposals for such a mechanism — the Goertler type mechanism (e.g. Sreenivasan 1988) and the nonlinear mechanism based on direct resonances (Jang, Benney and Gran 1986), for example — have been made, but none of these provides actual demonstration of a complete regeneration cycle. We have been able to show that the rolls are regenerated by the nonlinear development of an instability of the spanwise modulated shear flow, which is an instability of the streaks and mean shear, $U(y,z)$. Furthermore,

[2] For small times $t$ following the introduction of streamwise rolls on a parallel shear flow profile $U(y)$, one has $\overline{uv} \sim -t\,\overline{v^2}\,dU/dy$.

we have demonstrated this mechanism as a part of a complete, realized, *self-sustaining process*, in which streamwise rolls redistribute the mean shear to create streaks whose wake-like instability nonlinearly maintains the rolls.

Our approach has been threefold, consisting of controlled numerical simulations, stability analyses and low-order dynamical systems modeling. First, we tested the validity of our proposed process by tracking equilibrated turbulent solutions to a smaller computation box, i.e., to smaller Reynolds numbers for the three Reynolds numbers based on the largest length scales in each direction (Waleffe, Kim & Hamilton 1993). This led to an organization of the turbulent flow that settled onto the proposed coherent process, with all "inactive motions" removed by viscosity at small scales and forbidden by the small box at large scales. The self-sustaining process emerged spontaneously from this turbulent-solution tracking procedure (Waleffe *et al.* 1993, Hamilton *et al.* 1995). We sometimes refer to the resulting flow as "maximally constrained turbulence," but this flow is so organized that, in fact, it corresponds to the discovery of a periodic — in space and nearly in time — solution of the Navier-Stokes equations with plane Couette flow boundary conditions.

We separated the process into three phases, and studied each phase through a series of suitably altered computations (Hamilton *et al.* 1995), as well as through a stability analysis of spanwise-varying shear flows (Waleffe 1995a). The constrained simulations fully isolated the self-sustaining process (SSP), thereby demonstrating its continued existence independent of any other external influence such as the interaction with the outer flow. At the lowest Reynolds number at which it is self-sustaining, the process occupies the full width of the channel in plane Couette flow. The lowest Reynolds number for self-sustenance is about 350 in plane Couette flow (based on the 1/2 shear layer width and the 1/2 velocity difference across the shear layer), and thus matches well with the observed critical Reynolds number $R_c$ for transition in this flow. In Poiseuille flow, we expect two sets of streamwise rolls, one in each half of the channel. Hence, we expect an $R_c \approx 1400 = 4 \times 350$ in that flow (based on the shear layer width and the velocity difference across it) — slightly less than 1400 accounting for the absence of no-slip at the centerline — and that value is also close to the observed $R_c$ in plane Poiseuille flow.

Our position is that before tackling a high Reynolds number turbulent boundary layer, we should first understand the process responsible for the finite amplitude bifurcation of shear flows at low Reynolds number. This, of course, is the realm of transition studies that typically consists of follow-

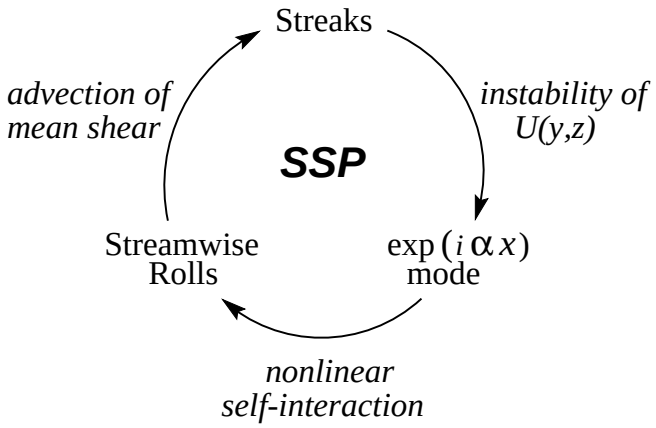


Figure 1: The three phases of the SSP.

ing the evolution of various special disturbances added to the laminar flow. Our approach was instead to come from the turbulence side of the problem by tracking turbulent solutions down to the critical Reynolds number in order to determine what state the flow transitions to, and how it self-maintains away from the laminar state. In this limit of small, but larger than critical, Reynolds number, one can rigorously separate the "active motions," or *coherent structures*, from the "inactive motions" (cf. preface to this monograph). We hypothesized that the coherent structures observed in turbulent boundary layers would be the principal surviving dynamical elements at transitional Reynolds numbers. This was indeed the case.

In the following, we first review the main ingredients of our SSP and the results of the low-order model. We then discuss the applicability of our results and offer some speculations about their relevance to higher Reynolds number turbulent boundary layers.

# 2 The Self-Sustaining Process (SSP)

In this section, we briefly review the three phases of our SSP, which have already been described in some details in Hamilton *et al.* (1995), Waleffe (1995a), and Waleffe (1997). We can view the process as composed of three main phases consisting of (i) the redistribution of the mean shear by streamwise rolls to create streaks, (ii) the wake-like instability of the streaks, and (iii) the regeneration of streamwise rolls from the nonlinear development of the streak instability (fig. 1; see also fig. 2 of Hamilton *et al.* 1995).

## 2.1 Formation of streaks

This is the simplest phase of the process that consists of redistribution of streamwise momentum by streamwise rolls. For $x$-independent flows, the wall-normal and spanwise velocities, $V(y,z)$, $W(y,z)$, respectively, that form the streamwise rolls, decouple from the streamwise velocity $U(y,z)$ (Waleffe 1995a). Thus they have no energy source and decay slowly due to viscosity. However they lead to a strong redistribution in $y-z$ planes of the streamwise momentum $U$ provided by the forcing, as governed by the advection-diffusion equation

$$\frac{\partial U}{\partial t} + V\frac{\partial U}{\partial y} + W\frac{\partial U}{\partial z} = \frac{1}{R}\nabla^2 U + F(y) \tag{1}$$

where $F(y)$ is a steady deterministic forcing that drives the shear flow if the boundary conditions are homogeneous. For plane Couette flow $F=0$ and the flow is driven by the motion of the boundaries $U(y=\pm 1)=\pm 1$, while $F$ is a constant for Poiseuille flow. Variables are non-dimensionalized by the half-channel height and the wall-velocity in Couette flow.

It is clear from eqn. (1) that streamwise rolls of $O(1/R)$ and of the scale of the shear layer are sufficient to induce an $O(1)$ $z$-modulation of the streamwise velocity, as particles with near extreme momentum are advected to the regions of average momentum. Beyond this, there is little scale selection with respect to the spanwise wavenumber $\gamma$. There is perhaps a slight preference for $\gamma \approx 1.2$ that corresponds to the slowest decaying rolls. [3] The spanwise variations, $U(y,z)-\overline{U}(y)$, where the overbar denotes an average over $z$, are called *streaks* in reference to the streaky structures observed in turbulent boundary layers (Kline *et al.* 1967).

## 2.2 Instability of sheared streaks

The spanwise-varying shear flow $U(y,z)$ consists of bands of fast and slow fluid side by side, and there are many inflections arising from the shear in the $z$-direction. In analogy with the instability of wakes (e.g. Drazin & Reid 1981), one then expects two dominant types of inflectional instability of the streaks, a *fundamental sinusoidal* mode (fig. 2) and a *subharmonic "sinucose"* mode. There is also a *fundamental varicose* mode, but it is expected to be least unstable. The symmetries of those various modes have

[3] The viscous decay rate of streamwise rolls $V(y,z) = V(y)\cos\gamma z$, with $V(y) \propto \cos(py)/\cos p - \cosh(\gamma y)/\cosh\gamma$, is $C_\gamma/R = (p^2+\gamma^2)/R$ with $p$ the smallest positive root of $p\tan p + \gamma\tanh\gamma = 0$. The minimum $C_\gamma = 9.27$ at $\gamma = 1.2$.

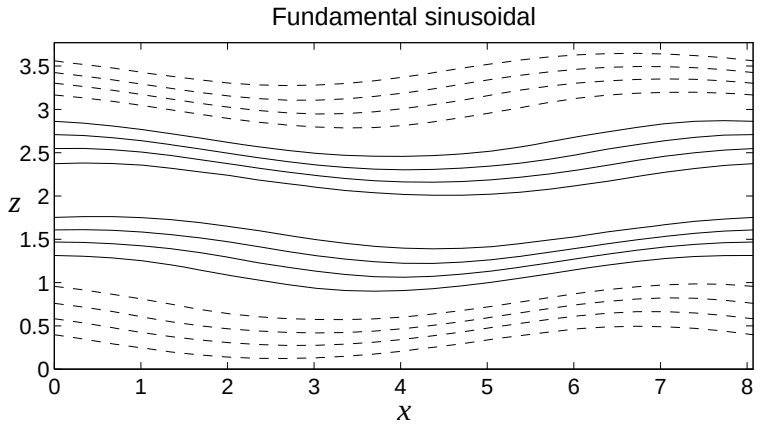


Figure 2: Fundamental sinusoidal mode of instability of streaks at $R = 400$. Contours of $u$ at 0.1292 increments at the centerline $y = 0$. Positive contours solid, negative contours dashed.

been discussed in Waleffe (1995a) and Waleffe (1997) and are illustrated in figs. 2 and 3 from direct numerical simulations (DNS). The fundamental mode was computed starting from the $U(y, z)$ profile at $R = 400$ in Waleffe (1995a) (described below) plus small random noise. The subharmonic was computed from a similar $U(y, z)$ profile at $R = 3000$ plus a small subharmonic perturbation (Waleffe 1995a). The subharmonic is a lot less unstable than the fundamental mode, and it was necessary to start with an initial field containing only the subharmonic mode and to use a higher Reynolds number to illustrate it in fig. 3.

For the near-wall region of turbulent flows the fundamental sinusoidal mode will lead to the typical staggered row of vortices as educed from turbulent data by Stretch (1990) and Jeong *et al.* (1996), while the subharmonic sinucose mode, and the fundamental varicose, would lead to symmetric *horseshoe*-like structures (e.g. Acarlar and Smith 1987). The data analysis by Stretch (1990), Jeong *et al.* (1996), and others showed that asymmetric structures are more typical than the symmetric horseshoes. This predominance is easily understood in terms of the wake instability analogy that favors the sinusoidal mode.

The streak instability is studied in Hamilton *et al.* (1995) using a full simulation code for the streaky flow obtained in the maximally constrained turbulent flow as well as related profiles. The linear stability problem for a spanwise varying shear flow $U(y, z)$ was formulated in Waleffe (1995a). The

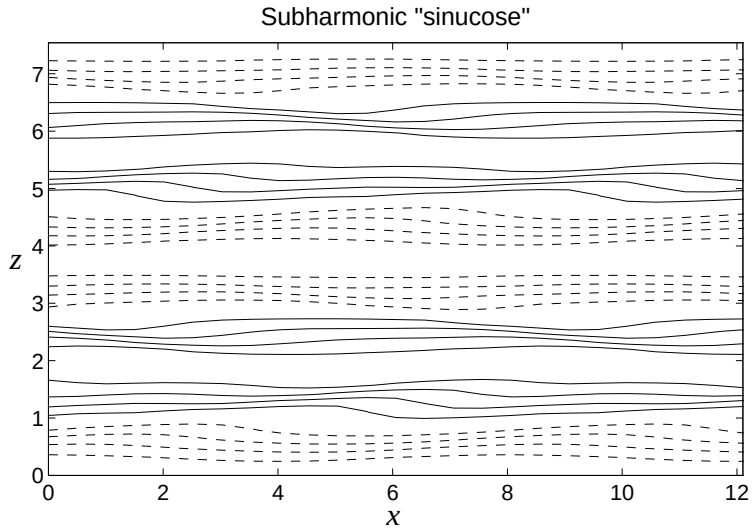


Figure 3: Subharmonic "sinucose" mode of instability of streaks at $R = 3000$. Contours of $u$ at 0.1417 increments at the centerline $y = 0$. Positive contours solid, negative contours dashed, 3/2 periods in $x$.

stability equations for the perturbations $v$, $\eta$ about the base flow $U$ read

$$\begin{aligned}\left(\frac{\partial}{\partial t}+U\frac{\partial}{\partial x}-\frac{1}{R}\nabla^2\right)\nabla^2 v+\left(\frac{\partial^2 U}{\partial z^2}-\frac{\partial^2 U}{\partial y^2}\right)\frac{\partial v}{\partial x}+2\frac{\partial U}{\partial z}\frac{\partial^2 v}{\partial x\partial z}&=\\ 2\frac{\partial^2}{\partial x\partial y}\left(w\frac{\partial U}{\partial z}\right),&\\ \left(\frac{\partial}{\partial t}+U\frac{\partial}{\partial x}-\frac{1}{R}\nabla^2\right)\eta=\left(\frac{\partial U}{\partial z}\frac{\partial}{\partial y}-\frac{\partial U}{\partial y}\frac{\partial}{\partial z}\right)v&\\ -\left(v\frac{\partial}{\partial y}+w\frac{\partial}{\partial z}\right)\frac{\partial U}{\partial z},&\end{aligned}\tag{2}$$

with the kinematic relation $(\partial^2/\partial x^2+\partial^2/\partial z^2)w=-\partial\eta/\partial x-\partial^2 v/\partial y\partial z$, where $\eta=\partial u/\partial z-\partial w/\partial x$ is the vertical vorticity and $\partial u/\partial x+\partial v/\partial y+\partial w/\partial z=0$ for incompressibility.

Eigensolutions of these linear stability equations are given in Waleffe (1995a) and Waleffe (1997) for the $U(y,z)$ profile obtained from the redistribution of the laminar plane Couette flow by streamwise rolls $V(y,z)=V(y)\cos\gamma z$, at $R=400$, after one quarter of the rolls turnover time $t=\pi h/(2V_{\max})$. This is approximately the time when momentum that was near the wall initially has been advected to the center of the channel, leading to

the largest streaks. The amplitude of the rolls $V_{\max}$ was chosen from the criterion that the rate of advection be of the order of the roll decay rate $V_{\max}/h \approx C_\gamma \nu/h^2$, thus selecting the weakest rolls that live long enough to create the strongest (and thus most unstable) streaks. In non-dimensional terms, the amplitude of the rolls is $V \approx C_\gamma/R$.

The stability of that $U(y,z)$ profile has been investigated with spectral methods using both no-slip ($u = v = w = 0$) and free-slip ($\partial u/\partial y = v = \partial w/\partial y = 0$) at the walls ($y = \pm 1$) for the eigenmodes, with little change in either the growth rate or the structure of the most unstable eigenmode. The growth rates are shown in fig. 4 for both types of boundary conditions. The no-slip results were compared with a full Navier-Stokes simulation code by starting from the $U(y,z)$ profile plus low amplitude random noise (fig. 2). The structure of the most unstable eigenmode in $y-z$ planes is plotted in fig. 5. The eigenmode consists primarily of spanwise velocity, as expected for the wake-like instability of the streaks. The superposition of the eigenmode with finite amplitude $\approx 0.15$ onto the base flow $U(y,z)$ is practically identical to the DNS figure 2.

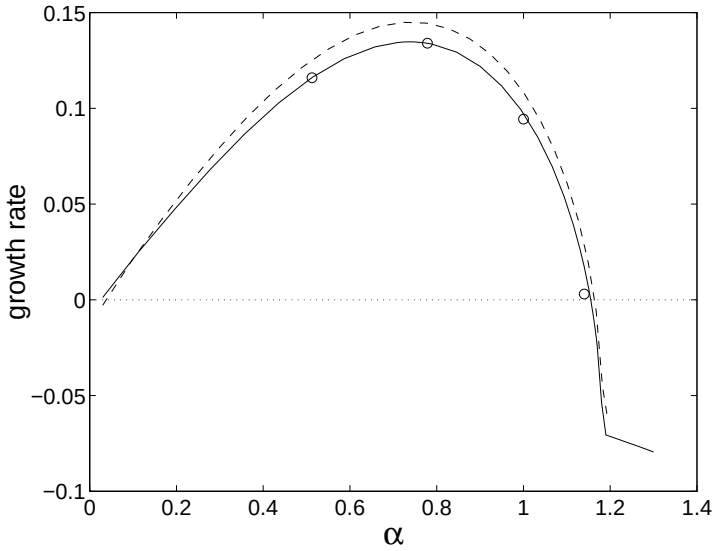


Figure 4: Growth rate of the unstable mode (fundamental sinusoidal) of a spanwise-modulated shear flow $U(y,z)$ with no-slip (solid) and free-slip (dash) boundary conditions, vs. streamwise wavenumber $\alpha$, for $\gamma = 5/3$, $R = 400$. Open circles are DNS results with no-slip.

The plot of growth rate versus streamwise wavenumber (fig. 4) has the shape characteristic of inflectional instabilities of smoothly varying profiles

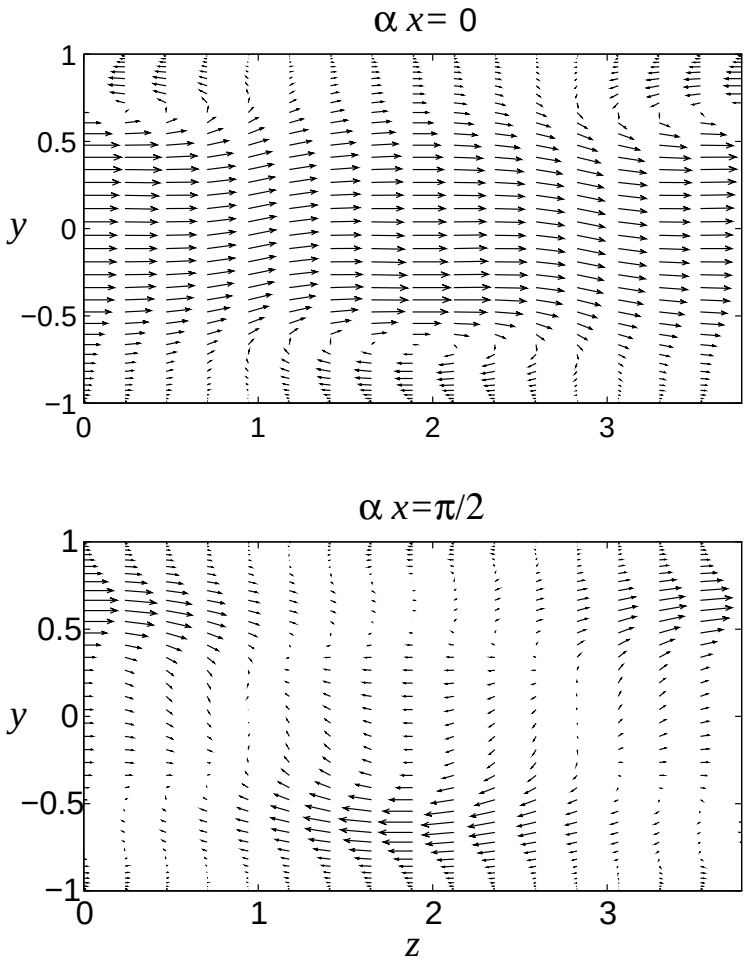


Figure 5: Eigenstructure of the fundamental sinusoidal mode (no-slip) for the instability of $U(y,z)$, consisting of a single $\exp(i\alpha x)$ Fourier mode, at $\alpha x = 0$ and $\alpha x = \pi/2$.

(Drazin & Reid 1981), for which there is a high wavenumber cutoff of the order of the typical wavenumber of the base flow. This has been illustrated (Waleffe 1995a, Waleffe 1997) by a low-order truncation for the stability of a purely spanwise shear flow $U_S \cos \gamma z$, in which the inviscid growth rate $\lambda$ has the expression

$$\lambda = \frac{|\alpha U_S|}{\sqrt{2}} \left( \frac{\gamma^2 - \alpha^2}{\gamma^2 + \alpha^2} \right)^{1/2},$$

where $\alpha$ is the streamwise wavenumber of the unstable mode. The band of unstable wavenumbers is $0 < \alpha < \gamma$. Viscous effects are easily included (see Waleffe 1997) and slightly shrink the unstable $\alpha$ range. The streak instability thus provides an upper bound on the streamwise wavenumber $\alpha$, but does not prominently favor any particular scale in the $z$-direction (wavenumber $\gamma$). Larger $\gamma$ implies more $y$-vorticity ($\partial U/\partial z$) in the streaks, and a larger instability growth rate, but it also implies more viscous damping and the streamwise rolls must then have a larger amplitude – and thus require more roll regeneration – to sustain the streaks.

Further study of the streak instability for various $U(y,z)$ profiles shows that the effect of the mean shear, $\overline{U}(y)$, is stabilizing: that is, the mean shear reduces the growth rates and the width of the unstable band of $x$-wavenumbers, mostly by lowering the upper cut-off wavenumber. The instability is thus clearly an instability of the streaks, $U(y,z) - \overline{U}(y)$, and is not enhanced but *reduced* by the presence of the mean shear. However, the mean shear $\overline{U}(y)$ is essential for feedback on the rolls, as discussed in the next subsection, in addition to being the source of energy for all fluctuations and for the streaks in particular. We note also that for some $U(y,z)$ profiles there is a second branch of unstable modes corresponding to traveling waves (the eigenvalues have a non-zero imaginary part) that extends to larger $\alpha$. Such branches are observed for the steady state $U(y,z)$ profiles obtained for the rolls used in Waleffe (1995a), for instance.

We emphasize here that it is an instability of the streaks, not of the rolls, that drives the process. This is illustrated by the analysis of the truncated model in Waleffe (1997) and Sect. 3 below. An instability of the rolls would provide another energy drain in addition to viscosity. The crucial element in shear flows is actually to identify the mechanism that *sustains* the rolls against the viscous decay. In the next subsection, we discuss how the streamwise rolls are regenerated by the $x$-dependent fluctuations that arise from the instability of the streamwise streaks.

## 2.3 Nonlinear feedback on streamwise rolls

Averaging the Navier-Stokes equations over the streamwise $x$-coordinate and then eliminating pressure and $\overline{W}^x$ through the incompressibility constraint yields the governing equation for the streamwise rolls $\overline{V}^x(y,z)$

$$\left(\frac{\partial}{\partial t} - \frac{1}{R}\nabla^2\right)\nabla^2\overline{V}^x(y,z) = \frac{\partial^3}{\partial y \partial z^2}(\overline{ww}^x - \overline{vv}^x) + \left(\frac{\partial^2}{\partial y^2} - \frac{\partial^2}{\partial z^2}\right)\frac{\partial}{\partial z}(\overline{vw}^x) \tag{3}$$

where the overbar-$x$, $\overline{(\cdot)}^x$, denotes an average over $x$ only. This is essentially an equation for the $x$-averaged streamwise vorticity $\overline{\omega_x}^x$ as $\nabla^2\overline{V}^x = -\partial\overline{\omega_x}^x/\partial z$.

This exact equation at once eliminates a candidate mechanism for the regeneration of streamwise rolls. It has been suggested that the streamwise rolls arise through the shearing by the mean flow $\overline{U}(y)$ of the vertical vortices arising from the roll-up of the vertical vorticity $\omega_y$ associated with streaks. This is not the case since such a mechanism would imply a forcing term resulting from the interaction between $U(y)$ and $\omega_y$, but there is no such forcing term in the $\overline{V}^x$ equation. Imagine a rotating stack of coins in a shear flow to represent $\omega_y$ vortices. The shear will displace the coins parallel to their plane thus generating streamwise vorticity $\omega_x$, but the latter does not correspond to streamwise vortices; no vertical velocity has been generated and $\omega_x$ results from the vertical shear of the spanwise velocity, $\partial w/\partial y$. The resulting $\omega_x$ has zero $x$-average.

Feedback on the streamwise rolls is more direct, but subtle, as its essential ingredients are intimately coupled with the instability of the *sheared* streaks. The mean shear plays an essential role for feedback by breaking the $y$-symmetry. This is illustrated by an intermediate fifth-order model deduced from a Galerkin projection (Waleffe 1997). That model shows that there are two independent modes — one odd and one even in $y$ — of instability of *pure* streaks (i.e. $U(y,z) = \cos\pi/2y\,\cos\gamma z$ in Couette and $U(y,z) = \cos\gamma z$ for the free-slip flow in Waleffe 1997), and that feedback on the rolls results from the nonlinear interaction between those two modes. The mean shear couples those odd and even modes of instability and correlates them such that feedback on the rolls is realized. Hence, although the basic instability results from the spanwise inflections, the latter alone are not sufficient to generate streamwise vortices. The mean shear intervenes at the level of the streak instability by shaping the unstable eigenstructure such that while its $\overline{uv}^x$ and $\overline{uw}^x$ Reynolds stress components extract energy from the spanwise modulated streamwise velocity $U(y,z)$ ((Hamilton *et al.*

1995), fig. 7), its $\overline{vv}^x$, $\overline{vw}^x$ and $\overline{ww}^x$ Reynolds stresses inject energy into streamwise rolls, eqn. (3) and fig. 6 (also, (Hamilton *et al.* 1995), figs. 4, 12 and 13). The nonlinear feedback is slightly dominated by $\overline{ww}^x$. The "nonlinear forcing" in fig. 6 was calculated by substituting the unstable eigenfunction (fig. 5) obtained from the eigensolver (Waleffe 1995a) into the right-hand side of eqn. (3).

Note that $\overline{V}^x(y,z)$ is generated even if absent initially at it results from the nonlinear interactions of $e^{i\alpha x}$ streak instability modes. Streamwise rolls can and have been generated by starting from the streaky flow $U(y,z)$ plus some small $x$-dependent fluctuations to trigger the streak instability with no rolls initially present.

The average streamwise vorticity $\overline{\omega_x}^x$ is simply related to $\overline{V}^x$ through $\nabla^2\overline{V}^x = -\partial\overline{\omega_x}^x/\partial z$, and thus fig. 6 is identical to fig. 13 in (Hamilton *et al.* 1995) modulo a quarter period shift in the $z$ direction. The nonlinear forcing is well-correlated with the original streamwise rolls and feedback is realized. The shape of the nonlinear forcing has an interesting double hump structure which suggests that it tends to create two sets of rolls, one near each wall. At low Reynolds numbers in Couette flow, however, the walls are close to each other so that the regenerated rolls merge into a single large roll occupying the whole channel. But the double hump structure of the nonlinear forcing suggests that two distinct vortices will be formed, one near each wall, at higher Reynolds number.

Physically, the conceptual picture of an *inclined* roll-up of the two-dimensional shear layer associated with the streamwise streaks, as in the generation of horseshoe vortices (Acarlar & Smith 1987), is probably a useful and valid visualization of both the streak instability and the feedback on the rolls. In our description of the SSP and its dynamics, we are led to distinguish between the $x$-dependent modes of instability of the streaks and their $x$-averaged nonlinear feedback on the rolls. In the full flow these two stages take the form of the staggered row of vortices for the fundamental sinusoidal mode of instability and of horseshoes vortices for the subharmonic sinucose mode. In the limit of low, transitional, Reynolds numbers, our "modal" view of the flow seems quite appropriate. At higher Reynolds numbers when interaction with the outer flow is present, the "structural" view of the flow may be more appropriate, but it is more difficult to describe mathematically.

With regards to the issue of scale selection, note that the second term on the right-hand side of (3), which contains the operator $\partial^2/\partial y^2 - \partial^2/\partial z^2$, changes its sign as the scales in the $y$ and $z$ direction cross over one an-

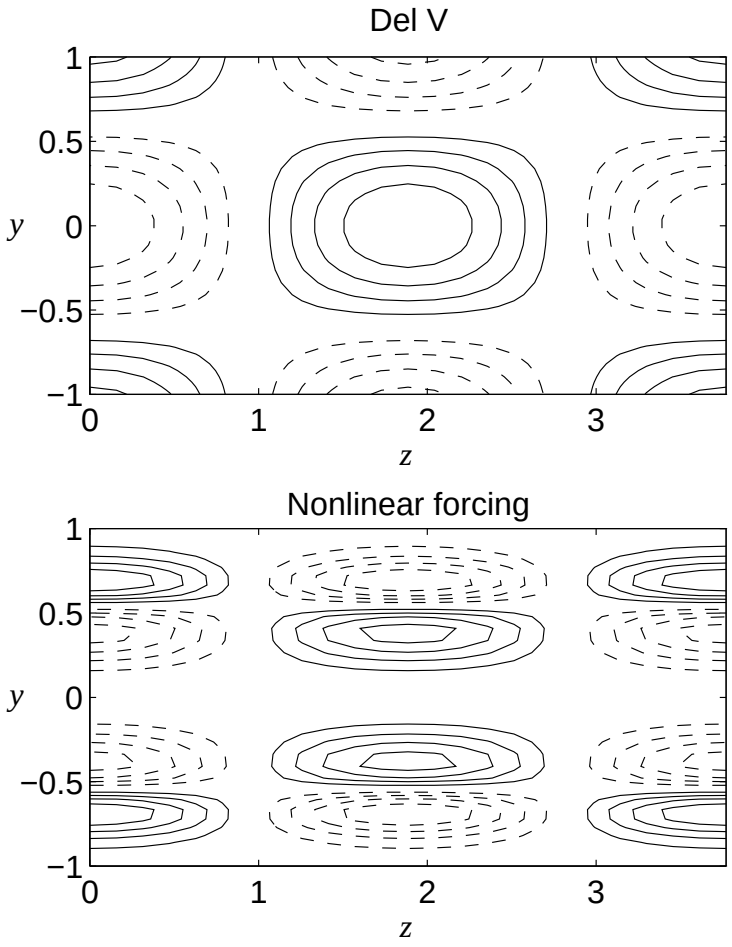


Figure 6: Feedback on streamwise rolls: top is $\nabla^2 \overline{V}^x$ for the pure streamwise rolls chosen to create $U(y, z)$ (Sect. 2.2); bottom is RHS of eqn. (3) resulting from nonlinear self-interaction of the streak eigenmode, fig. 5. Positive contours solid, negative contours dashed.

other. The form of the first term – a difference between $\overline{ww}^x$ and $\overline{vv}^x$ – perhaps also suggests such a flip in sign, after a scaling argument such as $\overline{ww}^x \sim \gamma^2/\beta^2\,\overline{vv}^x$. A change of sign of the right-hand side of (3) implies a switch from production to destruction of the rolls. Indeed a low-order model (Waleffe 1997) shows that feedback is possible only if $\gamma > \beta$, where $\beta$ is a characteristic $y$-wavenumber. Otherwise the rolls are actually destroyed by the nonlinear interaction of the $\exp(\pm i\alpha x)$ modes. This provides a lower bound for $\gamma$, while an upper bound is provided by viscosity as the viscous decay scales like $\gamma^2$. This is perhaps the more direct evidence of a spanwise scale selection. If $\gamma$ is too small, there is little or no feedback and little or no streak instability. If $\gamma$ is too large viscous decay dominates, as it stabilizes the streaks and the mean shear while requiring larger amplitude rolls to sustain the streaks and a larger amplitude streak instability to sustain the rolls. The competition between those various effects leads to a critical $\gamma$.

The three phases of the SSP, formation of streaks by streamwise rolls, streak instability and feedback on the rolls, are described by the three equations (1), (2) and (3), respectively. However, those equations are not complete to describe the interactions between the three phases. Equation (1) lacks the Reynolds stress terms $\partial\overline{uv}^x/\partial y + \partial\overline{vw}^x/\partial z$ that extract energy from $U(y,z)$ to sustain the growth of the streak instability. Equations (2) lack the interaction between the rolls $V(y,z)$ and the streak disturbance $(u,v,w)$ that extract energy from the latter to sustain the rolls. A complete low-order model of the SSP is discussed in the next section.

# 3 Low-order model

A low-order model of the SSP was first proposed (Waleffe 1995a, Waleffe 1995b), and later derived from the Navier-Stokes equations (Waleffe 1997). Taking advantage of the similarity between free-slip and no-slip boundary conditions for the basic streak instability, the model is derived for a $\sin\beta y$ shear flow, $|\beta y| < \pi/2$, with free-slip at the walls. That flow is best suited to low-order modeling. The model consists of four differential equations for the amplitudes of the mean shear $M$, of the streaks $U$, of the rolls $V$ and of the streak instability $W$. The corresponding modes are, up to some normalization constants, $(\sin\beta y, 0, 0)$ for the mean, $(\cos\gamma z, 0, 0)$ for the streaks, and $(0, \gamma\cos\beta y\,\cos\gamma z, \beta\sin\beta y\,\sin\gamma z)$ for the streamwise rolls. The streak instability mode, whose amplitude is $W$, is a three-dimensional velocity field represented by a combination of five Stokes modes (see Waleffe 1997).

The model reads

$$\begin{aligned}
\left(\frac{d}{dt}+\frac{\kappa_m^2}{R}\right) M &= \frac{\kappa_m^2}{R} - \sigma_u\, UV + \sigma_m\, W^2 \\
\left(\frac{d}{dt}+\frac{\kappa_u^2}{R}\right) U &= \sigma_u\, MV - \sigma_w\, W^2 \\
\left(\frac{d}{dt}+\frac{\kappa_v^2}{R}\right) V &= \sigma_v\, W^2 \\
\left(\frac{d}{dt}+\frac{\kappa_w^2}{R}\right) W &= \sigma_w\, U\, W - \sigma_m\, M\, W - \sigma_v\, V\, W
\end{aligned} \tag{4}$$

where all the $\sigma$ coefficients are positive. Analytic expressions for the coefficients are given in Waleffe (1997) for two slightly different choices for the streak instability mode. One choice requires $\gamma^2 - \beta^2 - \alpha^2 > 0$, while the other choice requires $\gamma^2 - \alpha^2 > 0$ and $\gamma^2 - \beta^2 > 0$; otherwise, instability of the streaks and/or feedback on the rolls are not possible. Model (4) preserves the global properties of the Navier-Stokes equations. The nonlinear quadratic interaction terms conserve the total energy, which evolves owing to the forcing and viscous dissipation only: $R\, d/dt(M^2 + U^2 + V^2 + W^2) = \kappa_m^2 M(1-M) - (\kappa_u^2 U^2 + \kappa_v^2 V^2 + \kappa_w^2 W^2)$. Unbounded growth cannot occur and a statistically steady state is possible only for $0 < M \leq 1$.

The physical effects and the three phases of the SSP discussed in Sect. 2 can be recognized in the model. The mean $M$ is maintained by the external forcing $\kappa_m^2/R$; the streaks $U$ originate from the $MV$ term, which corresponds to the redistribution of the mean shear by the streamwise rolls with feedback on the mean through the Reynolds stress, $-UV$; the streak instability $W$ grows exponentially through the $UW$ term and feeds the rolls $V$ through its nonlinear self-interaction $W^2$. Energy must then be extracted from $U$ and $W$ respectively, and this takes place through the $W^2$ term in the $U$ equation and the $VW$ term in the $W$ equation. As discussed in subsections (2.2) and (2.3), the mean shear influences the form of the streak instability and typically reduces its growth rate. This results in the $MW$ term in the $W$ equation and the corresponding $W^2$ in the $M$ equation.

The mean, $M > 0$, is linearly stable. Rolls with $V < 0$ are unstable to $W$ but cannot be sustained. Positive rolls $V > 0$ are stable and can be sustained through $W^2$. The only term that can extract energy from the mean $M$ is the $UV$ term provided $UV > 0$. Hence the only possible nonlaminar self-sustained solution corresponds to $U > 0$, $V > 0$. In that case energy can be transferred from the mean $M$ to the streaks $U$ through the

$MV$ term. The streak instability then gives rise to $W$ through the $UW$ term and the nonlinear self-interaction of the streak perturbation ($\sigma_v W^2$) sustains the rolls $V$. Note that $U$ and $V$ are amplitudes of particular streak and roll modes, respectively. That the SSP corresponds to $U > 0$, $V > 0$, simply results from a particular choice of phase in the definitions of the modes. Physically, the SSP corresponds to negative Reynolds stress $\overline{uv} < 0$ resulting from the streamwise streaks and rolls, and for every "ejection" (velocity fluctuations $u < 0$, $v > 0$), there is a "sweep" ($u > 0$, $v < 0$) half a period away in the $z$-direction. The term $\sigma_m W^2 > 0$ in the $M$-equation always puts energy back into the mean, hence the $\exp(i\alpha x)$ disturbances that originate from the streak instability lead to positive Reynolds stress. Those disturbances extract energy from the streaks $U(y,z) - \overline{U}(y)$ through their $x$-averaged-only Reynolds stresses, but actually put energy back into the mean $\overline{U}(y)$ through their $x$ and $z$ averaged Reynolds stress (see also fig. 7 in (Hamilton *et al.* 1995)).

Analysis of model (4) (Waleffe 1997) shows that there is a critical Reynolds number $R_{sn}$, at which a *saddle-node* bifurcation takes place. For $R > R_{sn}$ there are two steady solutions to (4) in addition to the laminar state $M = 1$, $U = V = W = 0$, one of which is an unstable saddle-point. The other solution, however, is not the usual stable node; instead, it is an *unstable node*. As the Reynolds number $R$ is increased, that unstable node soon turns into an unstable spiral that tightens: that is, it becomes less unstable as $R$ is increased further. For some values of the parameters (Waleffe 1997), this may lead to a *homoclinic bifurcation* at some $R = R_{hc} > R_{sn}$, which gives rise to a stable limit cycle.

That interesting dynamical behavior is illustrated in fig. 7. The saddle-node bifurcation at $R = R_{sn}$ introduces two new fixed points, a saddle and an unstable node (open circles), but most initial conditions still end up at the laminar fixed point (solid black dot), which is a stable fixed point and the only attractor for $R < R_{sn}$ (fig. 7(a), (b)). For $R$ slightly above $R_{sn}$, the unstable node turns into an unstable spiral (fig. 7(c)). As $R$ is increased, the spiral tightens and a homoclinic bifurcation takes place. This gives rise to a stable limit cycle, which is a new attractor (fig. 7(d)). Many initial conditions will now settle onto the periodic orbit instead of the laminar fixed point.

The low-order model thus offers some suggestions about the bifurcation of shear flows and a framework to understand how the various results and observations fit together. The two unstable steady solutions that arise through a saddle-node bifurcation at $R = R_{sn}$ correspond to the steady

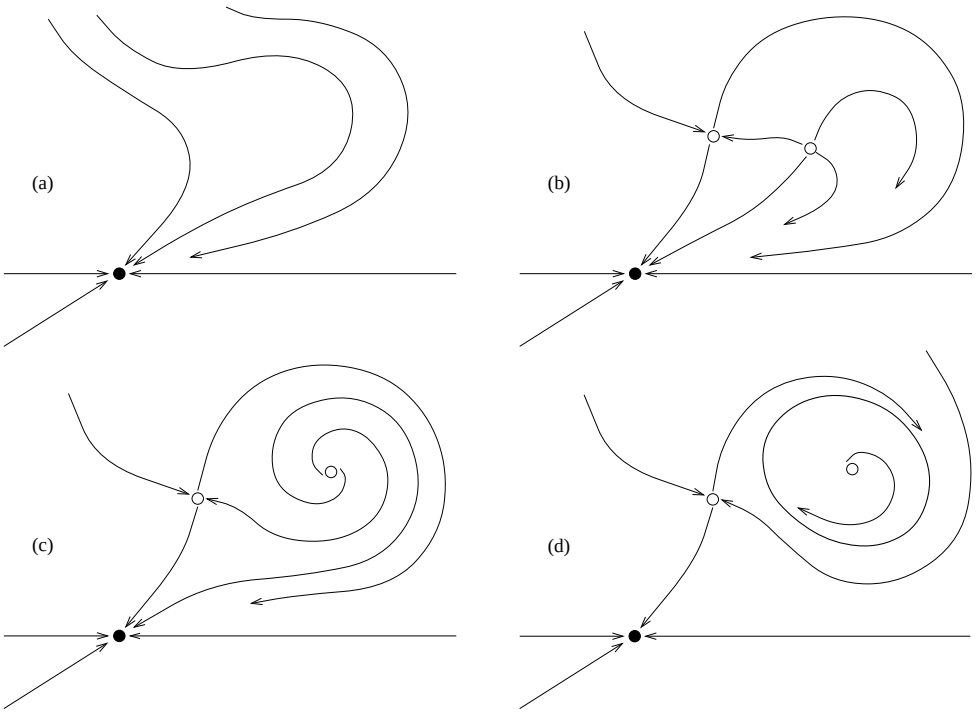


Figure 7: Phase plane illustration of some possible dynamics for model (4). The solid black dot is the stable laminar solution. The two open circles are the two new steady solutions. (a) $R < R_{sn}$: Laminar flow is global attractor and unique fixed point; (b) $R$ just above $R_{sn}$: two new fixed points have appeared, a saddle and an unstable node; (c) $R_{hc} > R > R_{sn} + \epsilon$: unstable node has turned into an unstable spiral; (d) $R > R_{hc}$: a stable limit cycle has appeared through a homoclinic bifurcation.

solutions computed by Nagata (1990), and shown unstable by Clever and Busse (1992), while the periodic solution that arises after the homoclinic bifurcation at $R = R_{hc} > R_{sn}$ corresponds to our solutions (Waleffe *et al.* 1993, Hamilton *et al.* 1995). From a practical point of view, the critical Reynolds number for transition is that corresponding to the homoclinic bifurcation, but from a geometric point of view, the saddle-node bifurcation is a necessary precursor to the homoclinic bifurcation (fig. 7). Note also that the unstable spiral fixed point could serve as an estimate of the average flow.

# 4 Discussion

Previous observations of near-wall turbulence structures have guided us towards the identification and isolation of a simple self-sustaining process described above. Although this is a definite step forward in our understanding of the underlying physics of turbulent boundary layers, there are many issues and questions that remain unresolved.

Our SSP leads to a well-organized motion with highly increased momentum transfer, but what happened to the disorder? By strongly constraining the flow at the large scales, we have been able to suppress almost completely the "inactive motions". Under those constraints, the SSP is very organized. In fact we have not observed any chaos in the low-order model of Sect. 3 for the parameter values we have considered so far. Our constrained DNS does look chaotic (Waleffe *et al.* 1993 fig. 5, Hamilton *et al.* 1995 fig. 3), and also shows some small-scale disorder. But with a bit more patience and fine-tuning of the box size it is plausible that we could have made these features to disappear. Of course no one has ever observed such spatially periodic states in an extended domain, even at low Reynolds number, suggesting that our process is *somewhat* unstable. By "somewhat," we mean here that these instabilities do not destroy the process completely but simply reduce its efficiency. The flow remains "close" to the organized SSP that may provide a good upper bound for the turbulent momentum transfer. Indeed, there are two aspects of turbulence. One is the disorder; the other is the increased momentum transfer. The SSP may be responsible for the increased momentum transfer, while secondary (and tertiary and quaternary, etc...) instabilities would be the roots of the disorder and what is commonly known as the "inactive motions".

Given the close connection between our SSP and the structures observed in the near-wall region, we contend that it is probably the main engine that drives shear flow turbulence. It is also probably the process that takes place inside turbulent spots, although the shape and dynamics of the spot boundary — the boundary between the laminar solution and our new self-sustained solutions — may be controlled by other processes. Indeed the shape of turbulent spots varies from one shear flow to another while the internal structure of various turbulent spots looks very similar, consistent with the above notion that the same SSP is the driving force inside turbulent spots.

The maximally constrained plane Couette flow considered here is the simplest configuration as far as the SSP is concerned. To extend the ap-

plicability of our SSP to the near-wall region in all wall-bounded turbulent flows, we need to investigate how it is affected when there is only one wall, as in boundary layers, or when the other wall does not provide an additional constraint, as in channel flow at sufficiently large Reynolds numbers so that the channel half-height is larger than the self-sustaining structure. A first step is to look at Poiseuille flow at a low Reynolds number, where we expect essentially two copies of this SSP, one in each half of the channel. Jimenez & Moin (1991) investigated a constrained channel flow (the so-called "minimal channel"), but the Reynolds numbers based on the channel half-height were large to allow larger-scale structures in the wall-normal direction, and consequently the SSP was less clearly discernible. A minimal channel flow at a Reynolds number barely large enough to support two copies of the SSP may lead to a simplified state similar to that considered here.

The other related issue is to study how the SSP depends on Reynolds number. As the Reynolds number increases, does a radically different process supersede the periodic and steady solutions based on the present SSP? This would strongly limit the relevance of the latter, but we do not think that is the case. Instabilities will arise and introduce disorder, but will not destroy the SSP. Perhaps these organized solutions develop an interesting nested structure, as in the upper bound solutions (Busse 1970), at higher Reynolds number, and they may even have a log-layer. We suspect, however, that the structure of the organized solutions at higher Reynolds number would be destroyed by instabilities, and that the SSP survives in an organized form only in the near-wall region. This is certainly what is suggested by the existing observations. The main question then is what happens away from the wall and how do the two regions interact? This is a perennial question, and much more work is needed to answer it. Characterizations of such organized solutions, however, seems to be a good, and new, starting point.

One of the most salient features of the wall-layer turbulence structure is the existence of a definite scale selection of about 100 wall units for the spacing of the wall-layer streaks. Jang *et al.* (1986) suggested that it corresponds to a scale at which there is a direct resonance between the Orr-Sommerfeld mode and Squire mode, in which case the latter undergoes a transient amplification. However, it was demonstrated in Waleffe *et al.* 1993 that the same linear mechanism, which is nothing but the velocity redistribution of Sec. 2.1, can lead to larger amplification of non-resonating modes and that there is no significant scale selection for this linear mechanism. Butler & Farrell (1993) introduced a cutoff time before which nonlinearity does not

affect the linear growth and after which it completely scrambles the flow and wipes out the linear growth. This is at best a strong simplification, but in any case, that nonlinear time scale remains as an adjustable external parameter. The linear mechanism thus does not explain the scale selection; instead, the scale-selection problem is simply transformed into a problem of time-scale selection.

Our analyses of the SSP show that there are scale constraints for its various phases. The typical wavenumbers must satisfy constraints of the kind $\alpha < \gamma$ for the streak instability to occur, and $\beta < \gamma$ for the nonlinear feedback on the rolls to occur. On the other end, if $\gamma$ is too large, viscous dissipation will prevent self-sustenance. However, it may not be feasible to come up with a simple argument for scale selection as the latter depends on *all* phases of the process as we discussed earlier (Waleffe *et al.* 1993, Hamilton *et al.* 1995). To illustrate this difficulty, let us put aside the scale-selection issue and ask about the relation between the amplitudes and the Reynolds number $R$ for self-sustenance in the low-order model eqn. (4). By balancing the viscous dissipation of each mode with its primary forcing term, i.e. $M \sim 1$, $U/R \sim MV$, $V/R \sim W^2$ and $W/R \sim UW$, we obtain the scalings $M \sim 1$, $U \sim R^{-1}$, $V \sim R^{-2}$ and $W \sim R^{-3/2}$ for the smallest amplitudes that may lead to self-sustenance. These are indeed the scalings of the lower branch saddle-point when $\sigma_m = 0$ (Waleffe 1995b). However, when $\sigma_m > 0$, the scalings of the lower branch are quite different: $M \sim$ const. $< 1$, $U \sim$ const. $> 0$, $V \sim R^{-1}$ and $W \sim R^{-1}$ (Waleffe 1997). Thus, it is difficult to deduce the appropriate scalings without actually calculating the bifurcated solutions. The scale selection is actually more related to the prediction of the critical Reynolds number $R_c$ for self-sustenance — rather than to asymptotic scaling — which is even more difficult to estimate without actual computation.

Our earlier suggestion Waleffe *et al.* (1993), which we reiterate here, is that the spanwise spacing of $\ell_z^+ = \ell_z u_\tau/\nu \approx 100$ is indeed a critical Reynolds number for self-sustenance, as demonstrated by the computations of Hamilton *et al.* (1995) and Jimenez & Moin (1991). In terms of the roll diameter $d$, which corresponds to one half of the streak spacing in the maximally constrained turbulence, the critical Reynolds number for self-sustenance is $d^+ = du_\tau/\nu \approx 50$. This roughly corresponds to the size of the buffer layer in turbulent boundary layers. The size of the buffer layer and the streak spacing would then correspond to the smallest scale that can have the SSP in turbulent boundary layers. At those small scales, there is little excess energy available for secondary instabilities or "inactive motions,"

but at the larger scales those instabilities can feed on and submerge the organized structures. This is perhaps the reason why the smallest scale that can have the SSP also corresponds to the most ubiquitous scale.

There is yet another possibility why $\ell_z^+ = 100$ is so conspicuous in turbulent boundary layers. As mentioned above the SSP defines the critical scale below which no self-sustenance is possible. All scales larger than the critical scale have the SSP. However, the resulting structure of the rolls, streaks and mean-shear in turbulent boundary layers is such that the energy transfer from the mean (the ultimate source of energy for all disturbances) is most efficient at $\ell_z^+ \approx 100$. In this sense, $\ell_z^+ \approx 100$ is not only the critical scale below which no SSP is supported, but also the dominant scale at which the energy transfer from the mean is most efficient. In an attempt to substantiate this argument, we examined the energy transfer from the mean to various $x$-independent spanwise scales using the channel DNS database of Kim *et al.* (1987). The energy transfer to $\widehat{u}(0,\gamma)$, where $\widehat{\ }$ and $\gamma$ denote a Fourier-transformed quantity and the spanwise wavenumber, respectively, from the mean shear is $\widehat{u}(0,\gamma)\widehat{v}(0,\gamma)dU/dy$, and hence, the efficiency of this transfer depends on the shapes of the rolls and the mean velocity profile resulting from the SSP. In fig. 8, this modal energy transfer, in terms of power density per nondimensionalized wavelengths, is shown as a function of distance from the wall. One sees that the streamwise rolls and streaks corresponding to $\ell_z^+ \approx 100$ are indeed the most significant contributors to energy extraction from *that particular mean*. Examination of a database obtained at a higher Reynolds number channel flow (approximately 7900 based on channel half-height and the centerline velocity instead of 3200) shows the same trend. It thus appears that the spanwise length scale corresponding to the observed mean streak spacing may be the spanwise scale at which the energy transfer due to the roll, streaks and mean shear of the SSP is most efficient.

# Acknowledgements

This work was initiated while the authors were affiliated with the Center for Turbulence Research at Stanford University/NASA Ames Research Center. J.K. is grateful to AFOSR (Program Manager, Dr. J. McMichael) and ONR (Program Manager, Dr. P. Purtell) for the partial support provided during the course of this work. Computer time was provided by the NAS Program of NASA Ames Research Center and the San Diego Supercomputing Center.

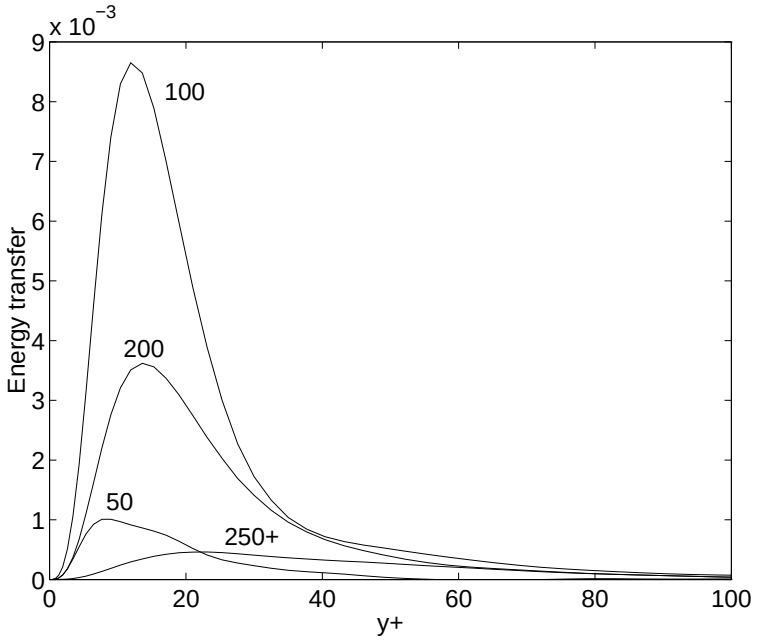


Figure 8: Energy transfer from the mean through the streamwise rolls and streaks, $\widehat{u}(0,\gamma)\widehat{v}(0,\gamma)dU/dy$ as function of the spanwise wavelength $2\pi/\gamma$. The curve labeled 250+ includes all transfer due to spanwise scales larger than 250.

# References


[1] Acarlar, M.S. & Smith, C.R. "A study of hairpin vortices in a laminar boundary layer," *J. Fluid Mech.* **175**, pp. 1-41 and 43-83 (1987).

[2] Benney, D.J. "The evolution of disturbances in shear flows at high Reynolds numbers," *Stud. Appl. Math.* **70**, 1-19 (1984).

[3] Busse, F.H. "Bounds for turbulent shear flows," *J. Fluid Mech.* **41**, 219-240 (1970).

[4] Butler, K. & Farrell, B. "Optimal perturbations and streak spacing in wall-bounded shear flow," *Phys. Fluids A* **5**, 774-777 (1993).

[5] Clever, R.M. and Busse, F.H. "Three-dimensional convection in a horizontal layer subjected to constant shear," *J. Fluid Mech.* **234**, 511-527 (1992).

[6] Drazin, P.G. & Reid, W.H., *Hydrodynamic Stability*, Cambridge University Press, 1981.

[7] Hamilton, J.M., Kim, J. & Waleffe, F. "Regeneration mechanisms of near-wall turbulence structures," *J. Fluid Mech.* **287**, 317-348 (1995).

[8] Jang, P.S., Benney, D.J. & Gran, R.L. "On the origin of streamwise vortices in a turbulent boundary layer," *J. Fluid Mech.* **169**, 109-123 (1986).

[9] Jeong, J., Hussain, F., Schoppa, W. & Kim, J. "Coherent structures near the wall in a turbulent channel flow," *J. Fluid Mech.* **332**, p. 185-214 (1997).

[10] Jimenez, J. & Moin, P. "The minimal flow unit in near-wall turbulence," *J. Fluid Mech.* **225**, 213-240 (1991).

[11] Joseph, D.D. & Tao, L.N. "Transverse velocity components in fully developed unsteady flows," *J. Appl. Mech.* **30**, 147-148 (1963).

[12] Kim, H.T., Kline, S.J. & Reynolds, W.C. "The production of turbulence near a smooth wall in a turbulent boundary layer," *J. Fluid Mech.* **50**, 133-160 (1971).

[13] Kim, J., Moin, P. & Moser, R. "Turbulence statistics in fully developed channel flow at low Reynolds number," *J. Fluid Mech.* **177**, 133-166 (1987).

[14] Kline, S.J., Reynolds, W.C., Schraub, F.A. & Rundstadler, P.W. "The structure of turbulent boundary layers," *J. Fluid Mech.* **30**, 741-773 (1967).

[15] Nagata, M. "Three-dimensional finite-amplitude solutions in plane Couette flow: bifurcation from infinity," *J. Fluid Mech.* **217**, 519-527 (1990).

[16] Robinson, S.K. "The kinematics of turbulent boundary layer structure," NASA TM 103859 (1991).

[17] Smith, C.R. & Metzler, S.P. "The characteristics of low-speed streaks in the near-wall region of a turbulent boundary layer," *J. Fluid Mech.* **129**, pp. 27-54 (1983).

[18] Sreenivasan, K.R. "A unified view of the origin and morphology of the turbulent boundary layer structure". In *Turbulence Management and Relaminarisation: Proc. IUTAM Symposium* (ed. H.W. Liepmann & R. Narasimha), pp. 37-61. Springer, 1988.

[19] Stretch, D.D. "Automated pattern eduction from turbulent flow diagnostics," *Annual Research Briefs-1990*, Center for Turbulence Research, Stanford University.

[20] Waleffe, F., Kim, J. & Hamilton, J.M. "On the origin of streaks in turbulent shear flows", in *Turbulent Shear Flows 8: selected papers from the Eighth International Symposium on Turbulent Shear Flows, Munich, Germany, Sept. 9-11, 1991*, F. Durst, R. Friedrich, B.E. Launder, F.W. Schmidt, U. Schumann, J.H. Whitelaw, Eds., pp. 37-49, Springer-Verlag, Berlin, 1993.

[21] Waleffe, F. "Hydrodynamic stability and turbulence: beyond transients to a self-sustaining process," *Studies in Appl. Math.*, **95**, 319-343 (1995a).

[22] Waleffe, F. "Transition in shear flows. Nonlinear normality versus non-normal linearity," *Phys. Fluids*, **7**, 3060-3066 (1995b).

[23] Waleffe, F. "On a self-sustaining process in shear flows," *Phys. Fluids*, **9**, 883-900 (1997).